

# Proton tracking for medical imaging and dosimetry

---

**J.T. Taylor<sup>a\*</sup>, P.P. Allport<sup>a</sup>, G.L. Casse<sup>a</sup>, N.A. Smith<sup>a</sup>, I. Tsurin<sup>a</sup>, N.M. Allinson<sup>b</sup>, M. Esposito<sup>b</sup>, A. Kacperek<sup>c</sup>, J. Nieto-Camero<sup>d</sup>, T. Price<sup>e</sup>, C. Waltham<sup>b</sup>**

<sup>a</sup>*Department of Physics, University of Liverpool, Oxford Street, Liverpool, L69 7ZE, U.K.*

<sup>b</sup>*Laboratory of Vision Engineering, School of Computer Science, University of Lincoln, Lincoln, LN6 7TS, U.K.*

<sup>c</sup>*Douglas Cyclotron, The Clatterbridge Cancer Centre NHS Foundation Trust, Clatterbridge Road, Bebington, Wirral, CH63 4JY, U.K.*

<sup>d</sup>*iThemba LABS, PO Box 722, Somerset West, 7129, South Africa*

<sup>e</sup>*School of Physics and Astronomy, University of Birmingham, Birmingham, B25 2TT, U.K.*

*E-mail: jtaylor@hep.ph.liv.ac.uk*

**ABSTRACT:** For many years, silicon micro-strip detectors have been successfully used as tracking detectors for particle and nuclear physics experiments. A new application of this technology is to the field of particle therapy, where radiotherapy is carried out by use of charged particles such as protons or carbon ions. Such a treatment has been shown to have advantages over standard x-ray radiotherapy and as a result of this, many new centres offering particle therapy are currently under construction - including two in the UK. The characteristics of a new silicon micro-strip detector based system for this application will be presented. The array uses specifically designed large area sensors in several stations in an  $x$ - $u$ - $v$  co-ordinate configuration suitable for very fast proton tracking with minimal ambiguities. The sensors will form a tracker capable of giving information on the path of high energy protons entering and exiting a patient. This will allow proton computed tomography ( $p$ CT) to aid the accurate delivery of treatment dose with tuned beam profile and energy. The tracker will also be capable of proton counting and position measurement at the higher fluences and full range of energies used during treatment allowing monitoring of the beam profile and total dose. Results and initial characterisation of sensors will be presented along with details of the proposed readout electronics. Radiation tests and studies with different electronics at the Clatterbridge Cancer Centre and the higher energy proton therapy facility of iThemba LABS in South Africa will also be shown.

**KEYWORDS:** Particle tracking detectors; Computerized Tomography (CT) and Computed Radiography (CR); Dosimetry concepts and apparatus; Instrumentation for particle-beam therapy.

---

\*Corresponding author.

---

## Contents

<b>1. Introduction</b>	<b>1</b>
<b>2. Tracker Design</b>	<b>2</b>
2.1 Tracker requirements	2
2.2 Sensor layout	2
2.3 ASIC design	3
<b>3. Sensor Characterisation</b>	<b>4</b>
3.1 Measurements with minimum ionising particles	4
3.2 Measurements with low energy protons	4
<b>4. Conclusions</b>	<b>5</b>

---

## 1. Introduction

The use of proton beams in radiotherapy is a well established technique that is increasingly being used as an option for patients who require radiotherapy [1]. Instrumental to the planning of any program of radiotherapy is a good imaging modality that can deliver accurate information on the patient's anatomy and in particular the accurate location of the target volume. For proton therapy, this is carried out by an x-ray CT scan from which the proton stopping power of the tissue can be derived and the necessary range of the treatment beam calculated. During this conversion from x-ray imaging to proton stopping power an uncertainty in the proton range is introduced, of order 1-3mm [2]. This arises from variations in density along the proton path [3] and inaccuracies in the excitation energy or  $I$ -value assumed for the tissue [4], as well as from the stopping power conversion method itself [5]. Uncertainties in the proton range increase the amount of dose delivered to the healthy tissue surrounding the cancer which can result in unwanted side effects and can prevent the treatment of cancers close to critical structures where if this uncertainty could be reduced, proton therapy would be an increasingly credible solution. These uncertainties could potentially be reduced if the stopping power of the beam could be calculated directly i.e. by using protons for imaging as well as for treatment [6]. In order to carry out this technique (referred to as proton computed tomography, or simply  $p$ CT), a device that can accurately measure the trajectory and energy loss of protons as they pass through an object for many different projections is needed [7] [8] [9]. The PRaVDA Consortium [10] aims to construct a prototype of the first fully solid state  $p$ CT scanner using silicon detectors for both the tracking and energy-range measurements of protons. This paper will focus on the silicon strip tracker, which builds upon technology developed for the high-luminosity LHC and is designed to demonstrate that high-precision directional information on the path of protons can be used in conjunction with a energy-range measurement to perform a  $p$ CT scan.

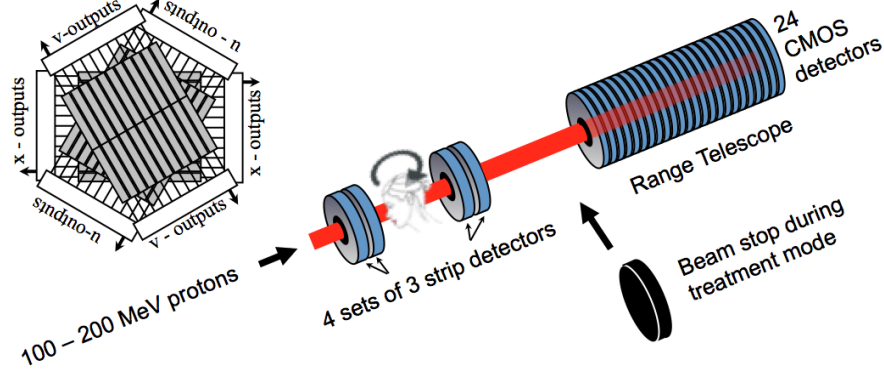


**Figure 1.** The proposed PRaVDA setup. Inset: Strip detector tracking station with  $x-u-v$  configuration.

## 2. Tracker Design

### 2.1 Tracker requirements

The PRaVDA silicon strip tracker is comprised of twelve detectors that form four tracking stations, two in front of the patient and two behind. In each station there are three detectors placed at  $60^\circ$  in an  $x-u-v$  configuration [11]. This allow for high fluences to be measured with minimal ambiguities (more than one possible hit location for each event) see Fig. 1, such that a reliable assessment of the size shape and fluence of a treatment beam can be made with a short acquisition time. The tracker will operate in two modes; treatment mode, and patient imaging or  $pCT$  mode. During the treatment mode a beam stop is placed in front of the range telescope to shield it from the high fluence, while the tracker is used to monitor the beam size, shape and fluence such that 1D & 2D dosimetry maps can be delivered to the user. During the imaging mode the whole system is read out at with a much lower fluence to ensure that as many protons as possible can be tracked and accurately measured in the range telescope, acquiring an image with the lowest possible dose.

### 2.2 Sensor layout

Each silicon strip detector is made from  $150\mu\text{m}$  thick  $n$ -in- $p$  silicon and has 2048 strips, 1024 read out on each side of the detector by eight ASICs. Each strip has a pitch of  $90.8\mu\text{m}$  and a length of  $4.8\text{cm}$  and its metal layer is capacitively coupled to its implant with a measured coupling capacitance of  $122\text{pF}$ . A polysilicon resistor, measured to be  $>2\text{M}\Omega$  connects each strip to the bias rail of the detector. The layout of the sensor can be seen in Fig. 2 with the active area of the detector shown to be  $93 \times 96 \text{ mm}^2$ . Detectors were fabricated by Micron Semiconductor Ltd. [12] with technology choices following closely those taken for the upgrade of the ATLAS experiment at the high-luminosity LHC in order for the sensor to be radiation hard in a clinical environment up to doses of around  $5 \times 10^{15} \text{ n eq/cm}^2$  [14][15].

Eighteen detectors have been received and tested so far, each with a nominal thickness of  $150\mu\text{m}$ . The depletion voltage is  $\sim 50\text{V}$  but detectors tested on the probe stations have been found to have leakage currents of  $\sim 10\mu\text{A}$  or less at six times this voltage. Such electrical properties are important not only for assessing the quality of the delivered detectors, but also in determining how

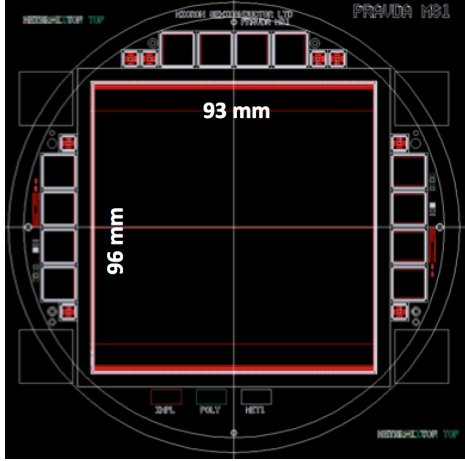


**Figure 2.** Wafer layout with active area labeled and test structures at the edges.

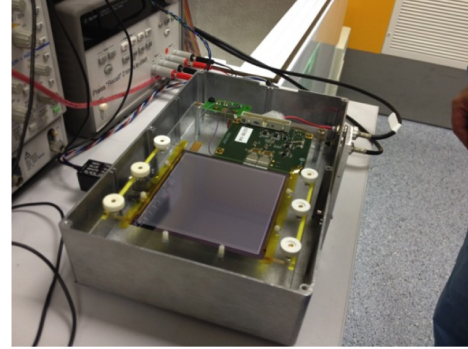


**Figure 3.** PRaVDA detector with partial readout for source and beam tests.

much heat will be generated by the tracker. This can impact on the noise in the electronic readout and what kind of cooling solution might be needed.

### 2.3 ASIC design

In order to readout the detectors in the tracker a new ASIC has been commercially designed by ISDI Ltd. [13] known as RHEA (Rapid High-speed Extended ASIC). It is a binary chip with a double threshold for each channel allowing for two particles per channel per readout frame and therefore high occupancy in the detectors, particularly useful for when the tracker is operated in treatment mode. Along with the  $x$ - $u$ - $v$  configuration of the tracking stations, the double threshold allows measurements of large area beams at high fluences with minimal ambiguities, which is important for fast beam quality assurance during treatment mode. For example, it was found using simple Monte Carlo methods that with up to 30 particles per frame there is an ambiguity rate of  $\sim 8\%$  whereas using orthogonal planes and a single threshold 2 particles per frame would give an ambiguity rate of 100%. In order to set appropriate ranges for the two thresholds, measurements with a smaller  $1\text{cm}^2$   $150\mu\text{m}$  thick sensor with similar strip pitch were taken using the BEETLE [16] ASIC and ALiBaVa readout [17] which delivers analogue data. Two measurements were taken for beam energies of 191 MeV and 60 MeV at iThemba LABS, South Africa, which are the maximum and minimum beam energies available from the accelerator and similar to the expected energies that the tracker will measure before and after the object (phantom) that will be imaged. This allowed an investigation of the size of proton clusters formed in the detector as a function of threshold for both energy settings. The results for this, as shown in Fig. 4 and Fig. 5, give the ranges of threshold 1 and threshold 2, which were chosen to be: 2,000 - 10,000  $e^-$ , and 20,000 - 160,000  $e^-$  respectively. The choice of specific thresholds values within these ranges will impact on the efficiency of the tracker and hence the total dose necessary to acquire an image. Data for selected thresholds will be discussed in Section 3, and typical cluster width plots with these thresholds can be seen in Fig. 7 and Fig. 8. The choice of threshold also has an impact on the precision of the tracking and is made such that the majority of events have a cluster width of one, minimising the

78 effect of tracking uncertainty on image quality, and also for compatibility with the RHEA read-out  
 79 constraints.

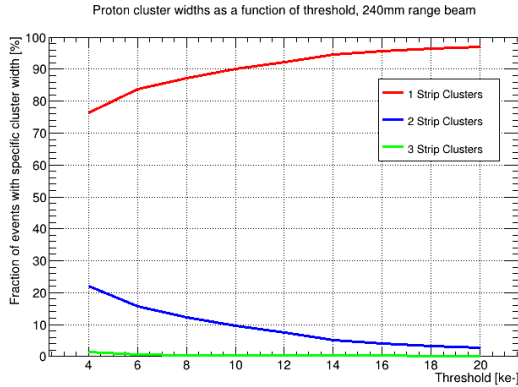


**Figure 4.** Cluster width as a function of threshold for a 191 MeV proton beam.

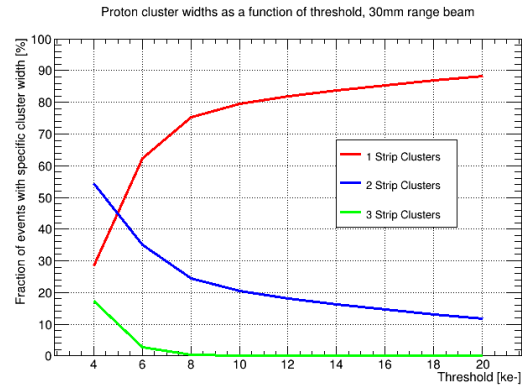


**Figure 5.** Cluster width as a function of threshold for a 60 MeV proton beam.

80 During treatment mode all channels will be read out every  $100\mu\text{s}$  to allow 1D and 2D beam  
 81 profile histograms to be made whilst in *pCT* mode it will be possible to read up to four channels  
 82 per ASIC with signal over threshold at 26 MHz (beam spill repetition rate at iThemba).

### 83 3. Sensor Characterisation

#### 84 3.1 Measurements with minimum ionising particles

85 In order to test the sensitivity of the detector to charged particles, 256 strips of a PRAVDA wafer  
 86 (12.5% of the detector) were wire-bonded to two BEETLE [16] ASICs and read out using the  
 87 ALiBaVa DAQ system [17]. The setup is shown in Fig. 3 inside a faraday cage where beneath  
 88 the sensor a plastic scintillator is placed to act as a trigger for the readout. The sensitivity of the  
 89 detector to minimum ionising particles was then tested in the lab using relativistic electrons from a  
 90  $^{90}\text{Sr}$  source. From this measurement an absolute calibration was also obtained by assuming that a  
 91 minimum ionising particle (MIP) produces a most probable value of  $80\text{ e-h pairs}/\mu\text{m}$  in silicon [11].  
 92 Since the wafer has a thickness of  $155\mu\text{m}$  we expect the Landau distribution to have an MPV of  
 93  $\sim 12,000\text{ e}^-$ . This data is shown in black in Fig. 6 with a threshold of  $5500\text{ e}^-$  applied to all strips  
 94 and fitted with Landau function convoluted with a Gaussian. The cluster width distribution for this  
 95 data is shown in Fig. 7 from which it can be seen that most events ( $>90\%$ ) are only one strip wide.

#### 96 3.2 Measurements with low energy protons

97 Using the same setup discussed above, the system was also tested using the Douglas Cyclotron at  
 98 the Clatterbridge Cancer Centre. This is currently the only clinical beam in the U.K. and has been  
 99 used for research as well as for the treatment of eye cancers for many years [18]. This experiment  
 100 allowed the response of the detector to be assessed for a clinical beam of 60 MeV protons. The  
 101 expected energy of protons emerging from the phantom and penetrating the second half of the  
 102 tracker (Fig. 1) is expected to be close to this energy from simulation studies in GEANT4 [19],

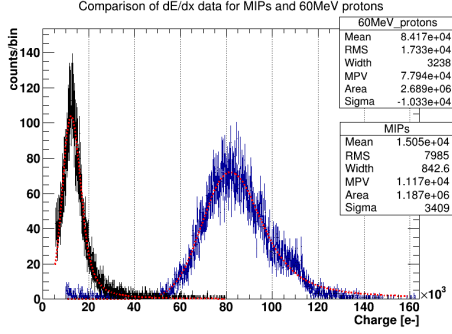


**Figure 6.** Energy loss of MIPs (black) and 60 MeV protons (blue) in a  $155\mu\text{m}$  PRaVDA detector.

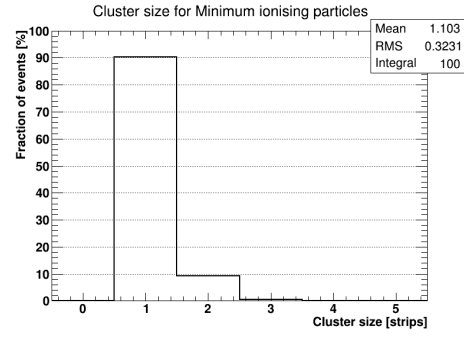


**Figure 7.** Cluster width for MIPs in a  $155\mu\text{m}$  PRaVDA detector with a threshold of  $5500 e^-$

and thus this experiment served as a way to test the sensors down to the lowest energy particles we expect to see in the final system. The energy loss of the protons is shown as the blue data in Fig. 6 with a threshold of  $10,000 e^-$  and with a fit using the same parameters as the data for MIPs. Fig. 6 represents data from both very high energy and very low energy particles and is thus a good source of information on the limits of the signals that we can expect to have in the final system. We will not be able to measure such quantities in the final system, due to the fact that the ASIC will operate in a binary fashion delivering only the addresses of the strips that are over the prescribed thresholds rather than the energy deposited in the strips themselves. The thresholds that are selected for the detectors in the tracker will have an impact on the efficiency of the system as well as the precision of the tracking. Such considerations are important as they will influence the dose that is necessary to acquire an image. The cluster width for 60 MeV protons is shown in Fig. 8 with a threshold of  $10,000 e^-$  and with a reduced single strip cluster fraction of  $\sim 70\%$ . The position distribution of the events is shown in Fig. 9 for a 3mm collimator.

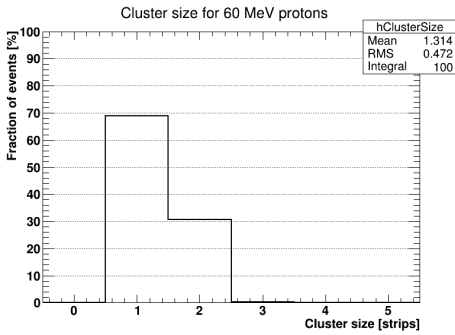


**Figure 8.** Cluster width for 60 MeV protons in a  $155\mu\text{m}$  PRaVDA detector with a threshold of  $10,000 e^-$

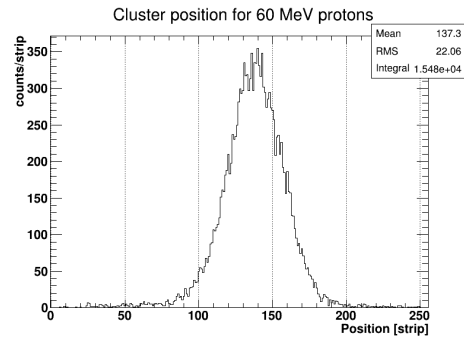


**Figure 9.** Position distribution for 60 MeV protons in a  $155\mu\text{m}$  PRaVDA detector with a threshold of  $10,000 e^-$

## 4. Conclusions

A new large area silicon micro-strip detector for medical applications has been presented along



with the general information on the ASIC that will be used for readout. The layout and operating modes of the tracker that the detectors will be assembled to make, has also been shown in Fig. 1 and discussed. The design of the PRAVDA detectors is informed by the technology choices made for detectors at the upgrade of the ATLAS experiment at the high luminosity LHC [14]. This has allowed the production of detectors that are very radiation hard [15] in order to provide the same signal outputs in a clinical beam for many years, delivering precise information on the trajectories of protons to aid with imaging and beam quality assurance.

## Acknowledgments

We would like to thank the members of the PRAVDA consortium, aSpect Systems GmbH, and ISDI Ltd. for their contributions and discussion of the results presented in this paper. We would also like to thank the operators and physicists at the iThemba LABS and the Clatterbridge Cancer Centre for producing and maintaining the proton beams that were used to make the measurements presented here.

This work was supported by the Wellcome Trust Translation Award Scheme, grant number 098285.

## References

- [1] D. Schulz-Ertner et al., *Particle Radiation Therapy Using Proton and Heavier Ion Beams*, *Journal of Clinical Oncology* **25** (2007) pp. 953-964
- [2] B Schaffner and E Pedroni, *The precision of proton range calculations in proton radiotherapy treatment planning: experimental verification of the relation between CT-HU and proton stopping power*, *Phys. Med. Biol.* **43** (1998)
- [3] Harald Paganetti, *Range uncertainties in proton therapy and the role of Monte Carlo simulations*, *Phys. Med. Biol.* **57** (2012)
- [4] Pedro Andreo, *On the clinical spatial resolution achievable with protons and heavier charged particle radiotherapy beams*, *Phys. Med. Biol.* **54** (2009)
- [5] Samuel España and Harald Paganetti, *The impact of uncertainties in the CT conversion algorithm when predicting proton beam ranges in patients from dose and PET-activity distributions*, *Phys. Med. Biol.* **55** (2010)
- [6] U. Schneider et al., *Proton radiography as a tool for quality control in proton therapy*, *Med. Phys.* **22** (1995)
- [7] U. Amaldi et al., *Construction, test and operation of a proton range radiography system*, *Nucl. Instrum. Methods Phys. Res. A* **629** (2011) pp. 337-344
- [8] M. Scaringella et al., *The PRIMA (PRoton IMAGING) collaboration: Development of a proton Computed Tomography apparatus*, *Nucl. Instrum. Methods Phys. Res. A* **730** (2013) pp. 178-183
- [9] H.F.-W. Sadrozinski et al., *Development of a head scanner for proton CT*, *Nucl. Instrum. Methods Phys. Res. A* **699** (2013) pp. 205-210
- [10] *The PRAVDA Consortium*: [www.pravda.uk.com](http://www.pravda.uk.com)
- [11] H. Spieler, *Semiconductor Detector Systems*, Oxford University Press Inc., New York 2009.

- 156 [12] Micron Semiconductor Ltd, 1 Royal Buildings, Marlborough Road, Lancing BN15 8UN, U.K.  
157 [www.micronsemiconductor.co.uk](http://www.micronsemiconductor.co.uk)
- 158 [13] ISDI Ltd. 7 Innovation House, Oxford Business Park South, Oxford, OX4 2JY, U.K.  
159 [www.isdicmos.com](http://www.isdicmos.com)
- 160 [14] ATLAS Collaboration, *Letter of Intent for the Phase-II Upgrade of the ATLAS Experiment (2012)*,  
161 *CERN-LHCC-2012-022. LHCC-I-023*
- 162 [15] M. Moll, *RD50 Status Report 2009/2010 - Radiation hard semiconductor devices for very high*  
163 *luminosity colliders, CERN-LHCC-2012-010. LHCC-SR-004*
- 164 [16] S. Löchner and M. Schmelling, *The Beetle reference manual for Beetle version 1.3/1.4/1.5*,  
165 *LHCb-2005-105. CERN-LHCb-2005-105 (2006)*
- 166 [17] [R. Marco-Hernández, A Portable Readout System for Microstrip Silicon Sensors \(ALIBAVA\), IEEE](#)  
167 [Nuclear Science Symposium Conference \(2008\) pp. 3201 - 3208](#)
- 168 [18] D.E. Bonnett et al., *The 62 MeV proton beam for the treatment of ocular melanoma at Clatterbridge*,  
169 *British Journal of Radiology* **66** (1993) pp. 907-914
- 170 [19] J. Allison et al., *Geant4 developments and applications, IEEE Transactions on Nuclear Science* **53**  
171 (2006) pp. 270-278